J Physiol 0.0 (2023) pp 1–21

Novel signalling pathways in nephrogenic syndrome of inappropriate antidiuresis: functional implication of site-specific AQP2 phosphorylation

Maria Venneri[1], Vanessa Vezzi[2], Annarita Di Mise[1], Marianna Ranieri[1], Mariangela Centrone[1], Grazia Tamma[1], Lene N. Nejsum[3] and Giovanna Valenti[1]

[1]*Department of Biosciences, Biotechnology and Environment, University of Bari Aldo Moro, Bari, Italy*
[2]*National Center for Drug Research and Evaluation, Istituto Superiore di Sanità, Rome, Italy*
[3]*Department of Clinical Medicine, Aarhus University, Aarhus, Denmark*

Handling Editors: Peying Fong & Rajini Rao

The peer review history is available in the Supporting information section of this article (https://doi.org/10.1113/JP284039#support-information-section).

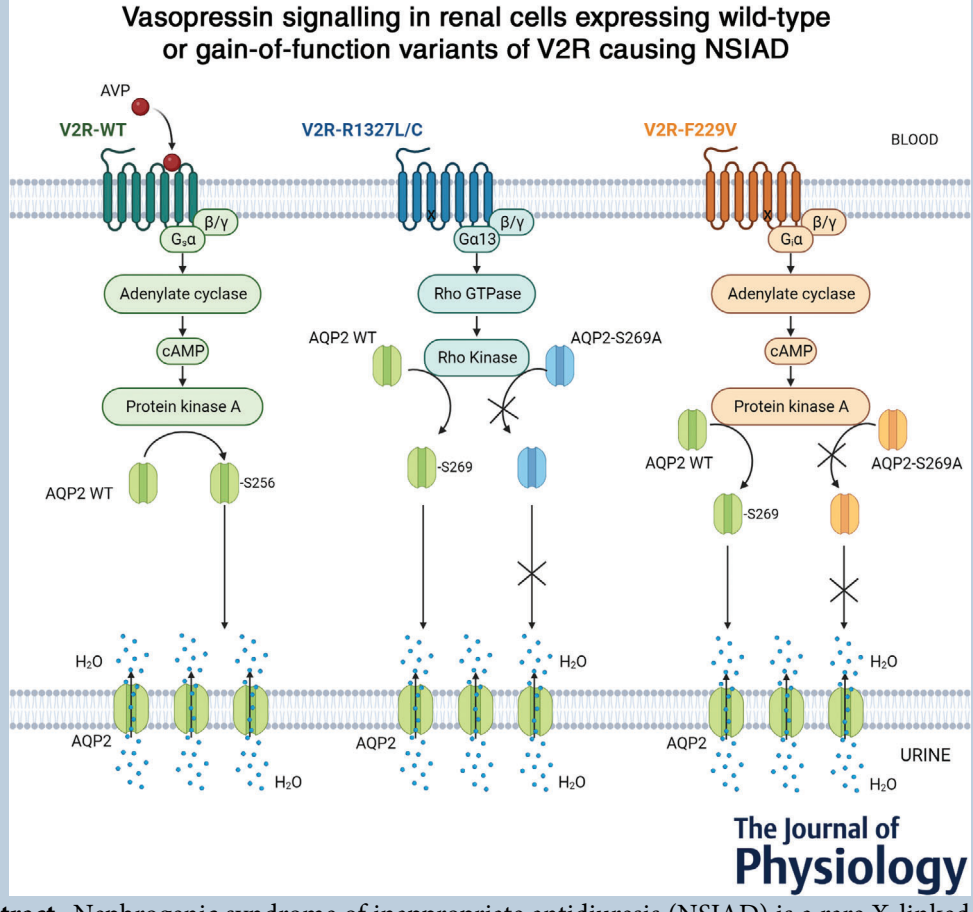

Abstract Nephrogenic syndrome of inappropriate antidiuresis (NSIAD) is a rare X-linked disease caused by gain-of-function mutations of arginine vasopressin receptor 2 (V2R). Patients with NSIAD

This article forms part of the 'Aquaporins in Health and Disease' symposium held at Copenhagen in September 2022, and organised by Robert Fenton.

DOI: 10.1113/JP284039

are characterized by the inability to excrete a free water load and by inappropriately increased urinary osmolality despite very low levels of plasma vasopressin, resulting in euvolaemic hyponatraemia. To dissect the signalling downstream V2R constitutively active variants, Flp-In T-REx Madin-Darby canine kidney (FTM) cells, stably transfected with V2R mutants (R137L, R137C and F229V) and AQP2-wt or non-phosphorylatable AQP2-S269A/AQP2-S256A, were used as cellular models. All three activating V2R mutations presented constitutive plasma membrane expression of AQP2-wt and significantly higher basal water permeability. In addition, V2R-R137L/C showed significantly higher activity of Rho-associated kinase (ROCK), a serine/threonine kinase previously suggested to be involved in S269-AQP2 phosphorylation downstream of these V2R mutants. Interestingly, FTM cells expressing V2R-R137L/C mutants and AQP2-S269A showed a significant reduction in AQP2 membrane abundance and a significant reduction in ROCK activity, indicating the crucial importance of S269-AQP2 phosphorylation in the gain-of-function phenotype. Conversely, V2R-R137L/C mutants retained the gain-of-function phenotype when AQP2-S256A was co-expressed. In contrast, cells expressing the F229V mutant and the non-phosphorylatable AQP2-S256A had a significant reduction in AQP2 membrane abundance along with a significant reduction in basal osmotic water permeability, indicating a crucial role of Ser256 for this mutant. These data indicate that the constitutive AQP2 trafficking associated with the gain-of-function V2R-R137L/C mutants causing NSIAD is protein kinase A independent and requires an intact Ser269 in AQP2 under the control of ROCK phosphorylation.

(Received 18 November 2022; accepted after revision 10 February 2023; first published online 23 February 2023)
Corresponding author Giovanna Valenti: Department of Biosciences, Biotechnology and Environment, University of Bari Aldo Moro, Bari 70125, Italy. Email: giovanna.valenti@uniba.it

Abstract figure legend In physiological conditions, vasopressin binds to arginine vasopressin receptor 2 (V2R-WT) in principal cells of the collecting duct. Binding to the receptor activates the Gs protein, leading to production of intracellular cAMP as a consequence of activation of adenylate cyclase. This pathway causes phosphorylation of the aquaporin 2 (AQP2) at S256, resulting in AQP2 insertion in the luminal plasma membrane. In cells expressing V2R-F229, AQP2 is constitutively expressed in the luminal membrane in the absence of vasopressin stimulation. Cells expressing the constitutively active AQP2-F229V mutant and the non-phosphorylatable AQP2-S256A lost their gain-of-function phenotype, indicating that this mutant requires an intact S256 phosphorylation site for translocation. In cells expressing V2R-R137L/C, the receptor is instead coupled to Gα12/13, causing activation of the serine/threonine kinase Rho-associated kinase (ROCK), which is involved in S269-AQP2 phosphorylation. Disruption of the S269 phosphorylation site prevented the constitutive trafficking of AQP2 to the luminal plasma membrane, indicating that the gain-of-function phenotype depends on AQP2 phosphorylation at S269.

Key points

- Nephrogenic syndrome of inappropriate antidiuresis is caused by two constitutively active variant phenotypes of *AVPR2*, one sensitive to vaptans (V2R-F229V) and the other vaptan resistant (V2R-R137C/L). In renal cells, all three activating arginine vasopressin receptor 2 (V2R) variants display constitutive AQP2 plasma membrane expression and high basal water permeability.
- In cells expressing V2R-R137L/C mutants, disruption of the AQP2-S269 phosphorylation site caused the loss of the gain-of-function phenotype, which, in contrast, was retained in V2R-F229V-expressing cells.
- Cells expressing the V2R-F229V mutant were instead sensitive to disruption of the AQP2-S256 phosphorylation site.
- The serine/threonine kinase Rho-associated kinase (ROCK) was found to be involved in AQP2-S269 phosphorylation downstream of the V2R-R137L/C mutants.
- These findings might have clinical relevance for patients with nephrogenic syndrome of inappropriate antidiuresis.

Introduction

Arginine vasopressin (AVP) plays a key role in the control of water homeostasis through activation of arginine vasopressin receptor 2 (V2R; also known as AVPR2) on the basolateral membrane of epithelial cells in the kidney collecting duct (Fenton et al., 2013; Ranieri et al., 2019). Ligand binding activates V2R, stimulating adenylate cyclase and leading to elevation of cAMP levels and activation of protein kinase A (PKA), which phosphorylates AQP2 at Ser256 (AQP2-S256; Fushimi et al., 1997; Nielsen et al., 1993). This promotes the shuttling of intracellular vesicles containing AQP2 to the apical membrane and an increase of water permeability, inducing antidiuresis. The phosphorylation of AQP2 on Ser256 by cAMP-dependent PKA has been shown to be crucial for the vasopressin-induced cell-surface accumulation of AQP2 (Fushimi et al., 1997; Katsura et al., 1997). The relevance of this phosphorylation site for the regulation of AQP2 trafficking has been demonstrated by mutational analysis. The AQP2-S256A mutant, which cannot be phosphorylated by PKA or other kinases, does not translocate to the plasma membrane in response to cAMP-elevating agents (van Balkom et al., 2002), whereas the AQP2-S256D mutant, mimicking constitutive phosphorylation, resides in the plasma membrane, independent of the cAMP level (Hoffert et al., 2006). The conclusion from these data is that phosphorylation at S256 is necessary and sufficient to induce the trafficking of AQP2 to the plasma membrane. Subsequent studies have indicated that phosphorylation at S256 precedes phosphorylation of other serine residues within the AQP2 C-terminus (Hoffert et al., 2006; Moeller et al., 2010). Among these serines, phosphorylation of S269 is thought to be crucial for AQP2 membrane retention (Hoffert et al., 2008), and interestingly, recent studies highlight the importance of S269 phosphorylation in AQP2 trafficking independently of S256 phosphorylation (Ando et al., 2016; Cheung et al., 2019).

Several disorders associated with inactivation or activation mutations in *AVPR2* lead to alterations of free water excretion and urinary concentrating defects (Ranieri et al., 2019). Nephrogenic syndrome of inappropriate antidiuresis (NSIAD) is a rare disorder characterized by constitutive activation of the X-linked V2R that causes excessive water reabsorption, hyponatraemia and seizures (Carpentier et al., 2012; Erdélyi et al., 2015; Feldman et al., 2005). Feldman et al. (2005) and, subsequently, Carpentier et al. (2012) identified two mutations in codon 137 (R137L and R137C) and one mutation in codon 229 (F229V) of *AVPR2*, respectively.

Arginine 137, located in the DRY/H domain of the second intracellular loop, seems to play an important role in the stabilization of the V2R in both its active and inactive forms (Audet & Bouvier, 2012). The substitution of this arginine with leucine or cysteine might permit the adoption of an activated form of the receptor, independent of AVP binding (Powlson et al., 2016). In contrast, the substitution of phenylalanine 229 with valine shows constitutive cAMP accumulation and sensitivity to inverse agonist of V2R, and this can indicate an overactivation of the cAMP/PKA pathway (Carpentier et al., 2012). Previously, we have described constitutive plasma membrane localization of AQP2 in cells expressing the V2R-activating mutations V2R-R137L, V2R-R137C and V2R-F229V, which lead to a significant increase in basal osmotic water permeability compared with the wild-type (WT) V2R-WT-expressing cells (Ranieri et al., 2020; Fig. 1). In V2R-F229V-expressing cells, the constitutive AQP2 plasma membrane localization involves cAMP/PKA-dependent phosphorylation of S256. In contrast, V2R-R137L and V2R-R137C involve alternative PKA-independent signalling that results in AQP2 insertion into the plasma membrane independently of S256 phosphorylation but requiring S269 phosphorylation (Ranieri et al., 2020).

In the present work, using the phospho-mimicking mutants AQP2-S256A and AQP2-S269A, we evaluate the relevance of these phosphorylation sites in the constitutive AQP2 insertion into the plasma membrane associated with different V2R variants causing NSIAD. We show that the non-phosphorylatable AQP2 mutants at the S256 or S269 sites differentiate AQP2 distribution in a distinct manner based on the V2R mutant analysed. Moreover, this study highlights the importance of ROCK in the phosphorylation of AQP2 in V2R-R137L and V2R-R137C mutant-expressing cells. These findings might have clinical relevance for patients with NSIAD.

Maria Venneri I received my PhD in 'Functional and Applied Genomics and Proteomics' in 2021, at the University of Bari, Italy, under the supervision of Professor Giovanna Valenti. I focused on the vasopressin–aquaporin 2 pathway in nephrogenic syndrome of inappropriate antidiuresis (NSIAD). As part of this research, I established international collaboration with a prestigious institution, where I spent a few months to accomplish specific tasks for my PhD project. To extend my research, I plan to work on genetic and acquired disorders of the kidney. In the near future, by investigating the molecular mechanisms of NSIAD, I hope to identify new therapeutic approaches for this rare disease.

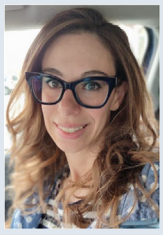

Methods

Chemicals and reagents

All chemicals were obtained from Merck (Merck KGaA, Darmstadt, Germany). Doxycycline hyclate (doxy; catalogue no. D9891, lot no. 069M4014V), desmopressin (dDAVP; catalogue no. V1005, lot no. 110M5055V) and forskolin (FK; catalogue no. sc3562, lot no. L1916) were purchased from Sigma (Sigma-Aldrich, Milan, Italy). Calcein-AM (catalogue no. C3100MP, lot no. 1034011) was bought from Molecular Probes (Life Technologies, Monza, Italy). Cell culture media and fetal bovine serum (FBS; catalogue no. 10270106) were from GIBCO (Life Technologies, Monza, Italy). Antibiotics and the ROCK inhibitor Y27632 (catalogue no. 688000, lot no. 3067661) were from Calbiochem. Super Signal West Pico Chemiluminescent Substrate (catalogue no. 34080, lot no. RE227122) and Super Signal West Femto Maximum Sensitivity Substrate (catalogue no. 34096, lot no. QH220582) were from Thermo Scientific (Rockford, IL, USA) and used for the ChemiDoc System (Bio-Rad Laboratories, Milan, Italy).

Antibodies

Mouse monoclonal antibody against AQP2-E2 (catalogue no. sc-515770, lot no. J0820) was purchased from Santa Cruz Biotechnology (Tebu Bio, Milan, Italy). Anti-phospho-MYPT1(Thr696) antibody was a component of the Rho-associated kinase (ROCK) activity assay (catalogue no. CSA001) purchased from Millipore (Merck KGaA, Darmstadt, Germany). Vasopressin receptor type 2 was detected using specific antibodies (anti-V2R; catalogue no. MBS8242744, lot no. CP1D10A) raised against a synthetic peptide corresponding to a sequence within the central region of human vasopressin V2 receptor from MyBioSouch (San Diego, CA, USA). Secondary goat anti-rabbit (catalogue no. A0545, lot no. 083M4752) or anti-mouse (catalogue no. A9044, lot no. 055M4818) horseradish peroxidase-coupled antibodies were obtained from Santa Cruz Biotechnologies (Tebu-Bio, Milan, Italy). Secondary goat anti-rabbit Alexa 488 and 647 conjugate antibodies were from Molecular Probes (Eugene, OR, USA).

Constructs

Human V2R wild-type (WT) and mutants (V2R-R137L, V2R-R137C and F229V) with c-Myc epitope in the N-terminal, expressed in pRK5 vector, were a gift from Professor Michel Bouvier (Université de Montréal, Montréal, Quebec, QC, Canada). Human c-Myc-tagged V2Rs (wild-type and mutants) were fused to the N-terminal of Rluc (Renilla luciferase) by linking each receptor sequence without its stop codon to Rluc cDNA through a decanucleotide linker peptide (GGGGSGGGGS) and cloned into puromycin resistance retroviral expression vector pQCXIP (Clontech). To generate pcDNA5/FRT/TO/(AQP2, AQP2-S256A or AQP2-S269A)myc constructs, *AQP2* cDNAs were amplified by PCR and cloned into pcDNA5/FRT/TO using the following primers: forward, 5′-GGCCGAATAGGGCCCAAGCGGCCGCGACTCTAG-3′; and reverse 5′-GGCCGAATAGGATCCGAGCTCGGTACCAAGCTT-3′. Both the empty plasmid (pcDNA5/FRT/TO/) and PCR products were digested with Apa1/BamHI restriction enzymes and ligated to obtain pcDNA5/FRT/TO/(AQP2, AQP2-S256A and AQP2-S269A)myc constructs. All sequences were verified by sequencing (GATC Biotech, Constance, Germany).

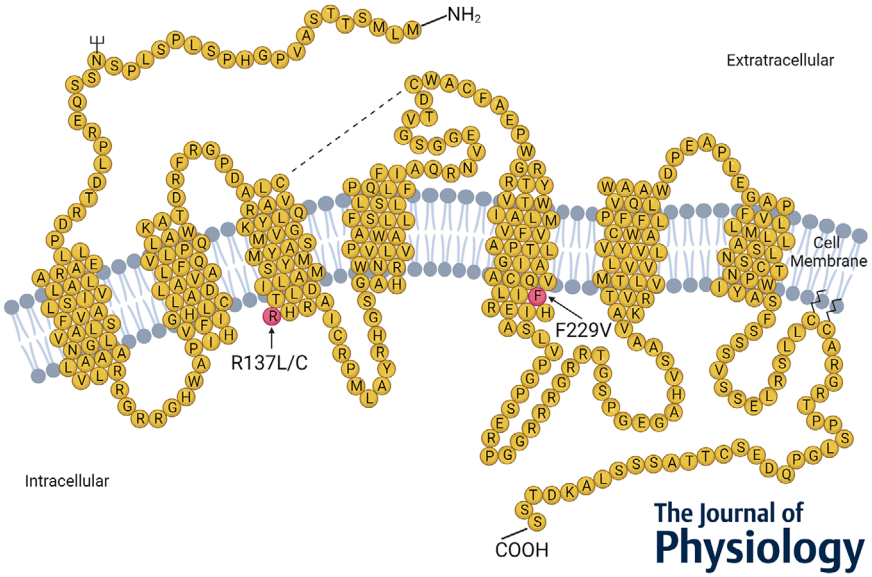

Figure 1. Diagram of the structure of arginine vasopressin receptor 2 in the cell membrane, showing the three mutations that cause nephrogenic syndrome of inappropriate antidiuresis
In yellow are shown the amino acid sequence of arginine vasopressin receptor 2 (V2R) in one-letter code and in red the three mutations, R137L/C and F229V.

Cell culture

For the generation of FTM cell lines, pcDNA5/FRT/TO/(AQP2, AQP2-S256A or AQP2-S269A)myc constructs were cotransfected into Flp-In T-REx doxycycline-inducible MDCK cells (Ernstsen et al., 2022; Holst & Nejsum, 2019; Nejsum et al., 2011) with Flp recombinase-encoding plasmid pOG44 (Invitrogen). The FTM cells were engineered permanently to express chimeric V2R-Rluc using the pantropic retroviral expression system by Clontech as described by Ranieri et al. (2019). Briefly, recombinant retroviruses expressing receptor–Rluc fusion proteins were prepared by transfection of GP2-293 packaging cells with different retroviral vectors using polyethyleneimine linear MW 25,000 Da (PEI). Cells were allowed to increase the viral titre for 48 h before collecting the virus-containing supernatants. The FTM cells were infected with the V2R-Rluc retroviruses in the presence of 8 μg/ml polybrene for 24 h and selected under puromycin (1 μg/ml). Then FTM cells were grown in Dulbecco's modified Eagle's medium, low glucose, pyruvate (DMEM 1×) supplemented with 10% (v/v) FBS (Thermo Fisher Scientific), 1% penicillin/streptomycin (Euroclone, Milan, Italy), 1 μg/ml puromycin (for V2R resistance; Thermo Fisher Scientific), 5 g/ml blasticidin S HCl (Gibco) and 100 g/ml hygromycin B (Invitrogen) at 37°C in air supplemented with 5% CO_2. Cells were kept at maximum 80% confluency and passaged every 2−3 days. Cells were induced with 2.5 ng/ml doxycycline for 48 h to express AQP2, AQP2-S256A or AQP2-S269A. After overnight treatment with indomethacin (50 M; ENZO Life Sciences) to suppress cAMP generation, cells were left in basal conditions or stimulated with 100 nM dDAVP for 1 h or with 50 M forskolin for 30 min to increase cAMP. Before stimulation, cells were starved for 3 h in medium with 50 M indomethacin but without FBS (starvation medium).

Cell preparations

For immunoblotting studies of plasma membrane fraction, FTM cells grown on 100-mm-diameter dishes (100% confluency) were lysed in cell fractionation buffer (20 mM NaCl, 130 mM KCl, 1 mM $MgCl_2$ and 10 mM Hepes, pH 7.5) in the presence of protease (1 mM phenylmethylsulfonyl fluoride, 2 mg/ml leupeptin and 2 mg/ml pepstatin A) and phosphatase (10 mM NaF and 1 mM sodium orthovanadate) inhibitors. The obtained lysates were centrifuged at 8,000 *g* for 20 min at 4°C to remove nuclear and heavy organelle debris. The supernatants were then centrifuged at 17,000 *g* for 1 h at 4°C. The obtained pellet consisted of a fraction highly enriched in plasma membranes, as confirmed by the abundance of the plasma membrane protein Na^+/K^+-ATPase (data not shown). The pellets were collected, resuspended in the isolation medium and used for immunoblotting studies.

For immunoblotting experiments in the total lysate, FTM cells were seeded onto 60-mm-diameter dishes (100% confluency) and were left in basal conditions. Subsequently, cells were homogenized in cell fractionation buffer in the presence of protease and phosphatase inhibitors, as above. The resulting homogenates were sonicated at 80% amplitude for 10 s. Cellular debris was removed by centrifugation at 12,000*g* for 10 min at 4°C. The supernatants were collected and used for immunoblotting experiments.

Gel electrophoresis and immunoblotting

Proteins were separated using 10 or 12% stain-free polyacrylamide gels (Bio-Rad Laboratories, Hercules, CA, USA) in reducing conditions. Protein bands were electrophoretically transferred onto Immobilon-P membranes (Merck Millipore, Milan, Italy) for western blot analysis, blocked in TBS–Tween-20 containing 3% bovine serum albumin (BSA), and incubated with primary antibodies overnight. Anti-AQP2 was used at 1:500 dilution, whereas anti-pMYPT1-T696 and anti-V2R were used at 1:250 dilution. Immunoreactive bands were detected with secondary goat anti-rabbit and goat anti-mouse antibodies conjugated to horseradish peroxidase-coupled antibodies obtained from Santa Cruz Biotechnologies (Tebu-Bio, Milan, Italy). Membranes were developed using Super Signal West Pico Chemiluminescent Substrate (Thermo Fisher Scientific) with the ChemiDoc System. Densitometry analysis was performed using Image Lab (Bio-Rad Laboratories, Milan, Italy). Data were analysed using GraphPad Prism (GraphPad Software, San Diego, CA, USA).

AQP2 immunolocalization by immunofluorescence

The FTM cells were grown on 20 mm glass coverslips, at maximum 70% confluency, and were fixed at room temperature with 4% paraformaldehyde in PBS for 20 min. The sample was permeabilized for 10 min with 0.1% Triton X-100 in blocking buffer containing 3% BSA in PBS, washed, and placed in blocking buffer for 20 min. Cells were then stained for AQP2 with 1:100 mouse anti-AQP2 for 1 h or V2R with 1:100 rabbit antiV2R for 1 h, washed three times with PBS, and stained with 1:1000 rabbit anti-mouse Alexa Fluor 647 (Invitrogen) or with 1:1000 donkey anti-rabbit Alexa Fluor 488 (Invitrogen), 8 μM Hoechst (to visualize nuclei) and 1:500 fluorescein isothiocyanate–phalloidin Alexa Fluor 488 (Invitrogen; to visualize actin filaments) for 1 h. Next, cells were rinsed three times with PBS and mounted on microscope slides using Glycergel Mounting Medium (Agilent

Technologies, Santa Clara, CA, USA) and imaged with a ×100 oil-immersion objective.

Microscopy and semiquantification of AQP2 localization

Imaging was performed using a Nikon EclipseTi-E inverted microscope equipped with ×60 and ×100 oil-immersion objectives, a Perfect Focus 3 system, a Zyla sCMOS5.5 Megapixel camera (Andor), and an Okolab heating system controlled by NIS Elements software from Nikon. The fluorescence illumination system was Cool LED-pE-300 white, and fluorescence filter sets were standard DAPI and GFP, TxRed and Cy5. All images were deconvolved with Huyjens Professional v.19.04 04 (Scientific Volume Imaging, The Netherlands; http://svi.nl). Image analysis was performed in ImageJ Fiji software (Schindelin et al., 2012). by placing regions in the plasma membrane between two adjacent cells. Quantification of AQP2, AQP2-S256A and AQP2-S269A in the membrane of cells was performed by line scanning, as previously described, in ImageJ Fiji software (Login et al., 2019, 2021).

Water permeability assay

Osmotic water permeability was measured by video imaging experiments. The FTM cells were grown on 40 mm glass coverslips (at maximum 60% confluency) and loaded with 10 μM membrane-permeable Calcein green-AM for 45 min at 37°C, in air enriched with 5% CO_2 in DMEM. Cells were left in basal conditions or stimulated with 100 nM dDAVP for 1 h. When indicated, cells were pretreated with the specific Rho kinase inhibitor (Y27632) at 10 μM for 30 min in basal conditions. The coverslips with dye-loaded cells were mounted in a perfusion chamber (FCS2 closed chamber system; Bioptechs, Butler, PA, USA), and measurements were performed using an inverted microscope (Nikon Eclipse TE2000-S microscope), equipped for single-cell fluorescence measurements and imaging analysis. The sample was illuminated through a ×40 oil-immersion objective (numerical aperture = 1.30). The Calcein green-AM loaded sample was excited at 490 nm. Emitted fluorescence was passed through a dichroic mirror, filtered at 515 nm (Omega Optical, Brattleboro, VT, USA) and captured by a cooled ECCD camera (CoolSNAP HQ; Photometrics, Tucson, AZ, USA). Fluorescence measurements, following iso-osmotic (304 mOsm/L; 140 mM NaCl, 5 mM KCl, 1 mM $MgCl_2$, 1 mM $CaCl_2$, 10 mM Hepes and 5 mM glucose) or hyperosmotic (404 mOsm/L; isosmotic solution with 135 mM mannitol added) solutions, were carried out using Metafluor software v.7.8.1.0 (Molecular Devices, San Jose, CA, USA). Calcein-AM is a non-fluorescent membrane-permeable dye, capable of quenching, which is converted to a green-fluorescent dye after acetoxymethyl ester hydrolysis, elicited by intracellular esterases. The exposure to a hyperosmotic solution leads to water efflux, causing cell shrinkage with a consequent increase in calcein concentration, quenching, and ultimate decrease of fluorescence intensity. The best-fitting τ values of the fluorescence intensity curve are proportional to the speed of water efflux and represent an indirect indication of the water permeability through AQP2 (Ranieri et al., 2019). The time course of cell shrinkage was measured as the time constant (Ki, per second).

Statistical analysis

One-way ANOVA followed by Tukey's multiple comparisons test was used for the statistical analysis. All values are expressed as means (SD). A difference of $P < 0.05$ was considered statistically significant.

Results

Cell surface localization of V2R-WT, V2R-R137L, V2R-R137C and V2R-F229V mutants in the Flp-In T-REx Madin-Darby canine kidney (FTM) cell line

To investigate the effect of different V2R mutations causing NSIAD on AQP2 trafficking, wild-type and mutated V2Rs (V2R-R137L, V2R-R137C and V2R-F229V) were stably transfected in the FTM cells, expressing *Rattus norvegicus* AQP2 and the different phospho-mimicking mutants AQP2-S256A and AQP2-S269A (Holst & Nejsum, 2019). In these cells, AQP2 expression was doxycycline inducible. Wild-type and mutated V2Rs (V2R-R137L, V2R-R137C and V2R-F229V) stably transfected in the FTM cells were analysed using two different approaches: western blotting and fluorescence microscopy.

Western blotting of plasma membrane-enriched fractions isolated from transfected cells, using monoclonal anti-V2R antibodies, revealed that, compared with V2R-WT, V2R-R137L, V2R-R137C and V2R-F229V exhibited a significant reduction in cell surface localization [Fig. 2*A* and *B*; V2R-WT, 1.000 (0.1275); V2R-R137L, 0.5939 (0.04473); V2R-R137C, 0.5911 (0.1901); and V2R-F229V, 0.4065 (0.06866); $n = 4$ independent experiments]. These data indicate that constitutive endocytosis was involved in the reduced steady-state cell surface localization of the three mutants (Rochdi et al., 2010). To assess the cellular distribution of the V2R mutants, fluorescence microscopy of FTM cells expressing the wild-type and mutated receptors was performed using monoclonal anti-V2R

antibodies. As shown in Fig. 2*C* and *D*, the V2R-WT was mainly localized at the cell surface, as indicated by the sharp fluorescence along the perimeter of the cells. With respect to V2R-WT, the V2R mutants exhibited reduced fluorescence, in agreement with the lower abundance in the plasma membrane and with western blotting data.

FTM cells expressing different V2R mutants were previously tested for temporal linear control of AQP2 expression 24 and 48 h after induction with 1, 2.5 or 5 ng/ml doxycycline. The treatment with 2.5 ng/ml doxycycline for 48 h showed a homogeneous AQP2 expression in the different cell lines, without any visible aggregation; hence, this concentration was chosen for the experiments (data not shown).

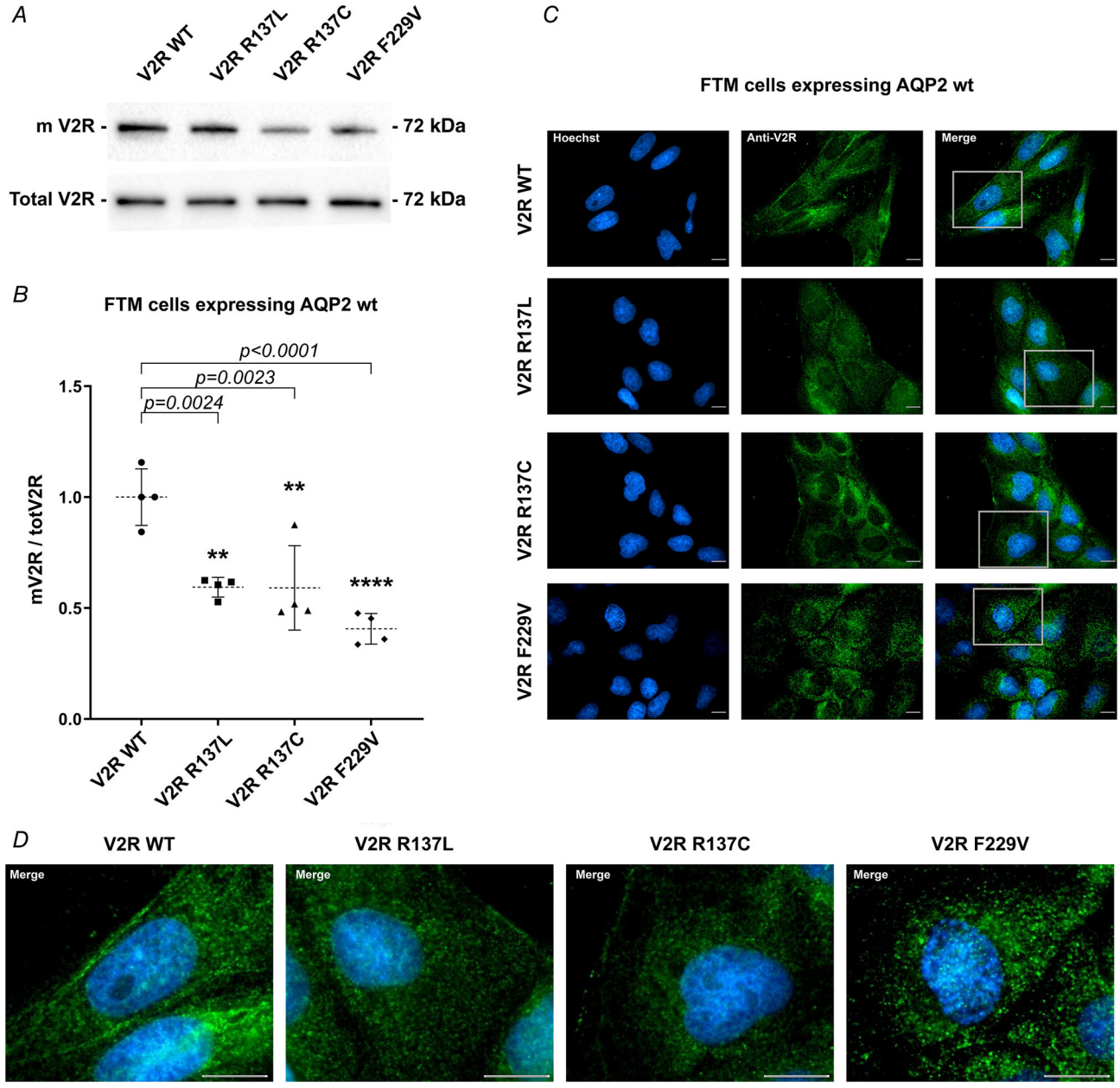

Figure 2. Cell surface localization of V2R-WT, V2R-R137L, V2R-R137C and V2R-F229V
A, representative western blots of the FTM cell lysate, showing membrane-bound arginine vasopressin receptor 2 (mV2R) and total arginine vasopressin receptor 2 (Total V2R) bands. *B*, densitometric analysis of bands of V2R abundance (mV2R) normalized to the total V2R (totV2R). The data are normalized to V2R-WT and are represented as the means (SD) of $n = 4$ independent experiments (**$P < 0.01$, ****$P < 0.0001$ *vs*. V2R-WT). *C*, V2R localization in FTM cells expressing AQP2-wt. The FTM cells were stained for V2R (green) and nuclei (blue) as indicated. Scale bars: 20 μm. *D*, the cells marked by grey squares in *C* were magnified ×10 to visualize the subcellular localization of the V2R. Scale bars: 20 μm.

AQP2-wt localization and water transport in cells expressing the V2Rs

In basal conditions, cells expressing V2R-WT AQP2 staining were mainly localized in intracellular vesicles (Fig. 3*A*, with ×10 magnification in Fig. 3*B*). Stimulation with either forskolin (FK) or desmopressin (dDAVP) resulted in a marked redistribution of AQP2 to the plasma membrane, confirming the functional expression of the receptor. In FTM cells expressing constitutively active mutants (V2R-R137L, V2R-R137C or V2R-F229V), AQP2 redistributed to the plasma membrane in the absence of hormonal stimulation (Fig. 3*A* and *B*), suggesting an agonist-independent receptor signalling.

The amount of AQP2 at the plasma membrane was semi-quantified using ImageJ Fiji software (Login et al., 2019), as previously described. With respect to basal conditions, in cells expressing V2R-WT and AQP2, the statistical analysis showed a significantly higher cell surface localization of AQP2 in cells treated with dDAVP or FK, and in the active V2R-R137L, V2R-R137C and V2R-F229V [Fig. 3*C*; V2R-WT, 1.000 (0.1401), $n = 5$ independent experiments, 44 cells tested; V2R-WT dDAVP, 2.190 (0.3658), $n = 5$ independent experiments, 49 cells tested; V2R-WT FK, 2.491 (0.4832), $n = 5$ independent experiments, 48 cells tested; V2R-R137L, 2.243 (0.4282), $n = 5$ independent experiments, 37 cells tested; V2R-R137C, 2.559 (0.4955), $n = 5$ independent experiments, 60 cells tested; and V2R-F229V, 2.565 (0.5629), $n = 5$ independent experiments, 46 cells tested].

Osmotic water permeability and AQP2 abundance in the plasma membrane

To assess the functional outcome of AQP2 translocation, the osmotic water permeability was measured in FTM cells expressing either the wild-type V2R or different receptor mutants.

As shown in Fig. 4*A* and *B*, in cells expressing the constitutively active mutants, the temporal osmotic response (indicated as $1/\tau$) was significantly higher compared with cells expressing the V2R-WT. As expected, dDAVP induced an increase in the osmotic water permeability in V2R-WT-expressing cells [V2R-WT, 1.000 (0.5510), $n = 4$ independent experiments, 122 cells tested; V2R WT dDAVP, 1.441 (0.7252), $n = 4$ independent experiments, 70 cells tested; V2R-R137L, 1.875 (0.7028), $n = 4$ independent experiments, 61 cells tested; V2R-R137C, 1.914 (0.8600), $n = 4$ independent experiments, 80 cells tested; and V2R-F229V, 1.641 (0.7014), $n = 4$ independent experiments, 101 cells tested].

Interestingly, the increase in osmotic water permeability was perfectly correlated with AQP2 translocation to the plasma membrane as assessed by semiquantitative western blotting analysis of plasma membrane-enriched preparations (Fig. 4*C* and *D*). Compared with cells expressing the V2R-WT, AQP2 abundance at the plasma membrane fraction was significantly higher in cells expressing the active V2R-R137L, V2R-R137C and V2R-F229V mutants [Fig. 4*D*; V2R-WT, 1.000 (0.1029); V2R-R137L, 2.281 (0.4995); V2R-R137C, 1.796 (0.6969); and V2R-F229V, 2.196 (0.3204); $n = 5$ independent experiments].

Role of pS/T269-AQP2 phosphorylation site in the cells expressing V2R-R137L and V2R-R137C mutants

We recently provided evidence of an alternative PKA-independent pathway that increased AQP2 membrane targeting and osmotic water permeability in collecting duct cells expressing the V2R-R137L and V2R-R137C mutants associated with an increase in pS/T269-AQP2, independently of p256 phosphorylation (Ranieri et al., 2020). To explore the relevance of the pS/T269-AQP2 phosphorylation site in these mutants, AQP2 localization and trafficking were performed in FTM cells expressing AQP2-S269A, which cannot be phosphorylated at S269, co-expressed in cells transfected with wild-type or V2R variants.

Widefield microscopy with deconvolution revealed that in V2R-R137L and V2R-R137C mutants, AQP2-S269A was constitutively located mainly in intracellular vesicles (Fig. 5*A* and *B*), indicating that phosphorylation at S/T269 is essential for the gain-of-function phenotype in V2R-R137L and V2R-R137C cells. In contrast, in cells co-expressing V2R-F229V mutant and AQP2-S269A, AQP2 was constitutively detectable on plasma membrane, indicating that the gain-of-function variant V2R-F229V does not require phosphorylation of AQP2 at S/T269 to promote AQP2 redistribution to the plasma membrane. Fig. 5*C* reports the statistical analysis of AQP2-S269A quantification on the plasma membrane in the different cell lines using the ImageJ Fiji software [V2R-WT, 1.000 (0.1689), $n = 3$ independent experiments, 20 cells tested; V2R-WT dDAVP, 1.413 (0.7281), $n = 3$ independent experiments, 25 cells tested; V2R-WT FK, 1.891 (0.4044), $n = 3$ independent experiments, 26 cells tested; V2R-R137L, 1.093 (0.1581), $n = 3$ independent experiments, 21 cells tested; V2R-R137C, 1.020 (0.2025), $n = 3$ independent experiments, 28 cells tested; and V2R-F229V, 1.425 (0.2374), $n = 3$ independent experiments, 12 cells tested].

In line with these data, functional studies demonstrated that the osmotic water permeability was significantly reduced in cells co-expressing AQP2-S269A and V2R-R137L or V2R-R137C. In contrast, cells co-expressing AQP2-S269A and the V2R-F229V had a significantly higher osmotic water permeability, reflecting

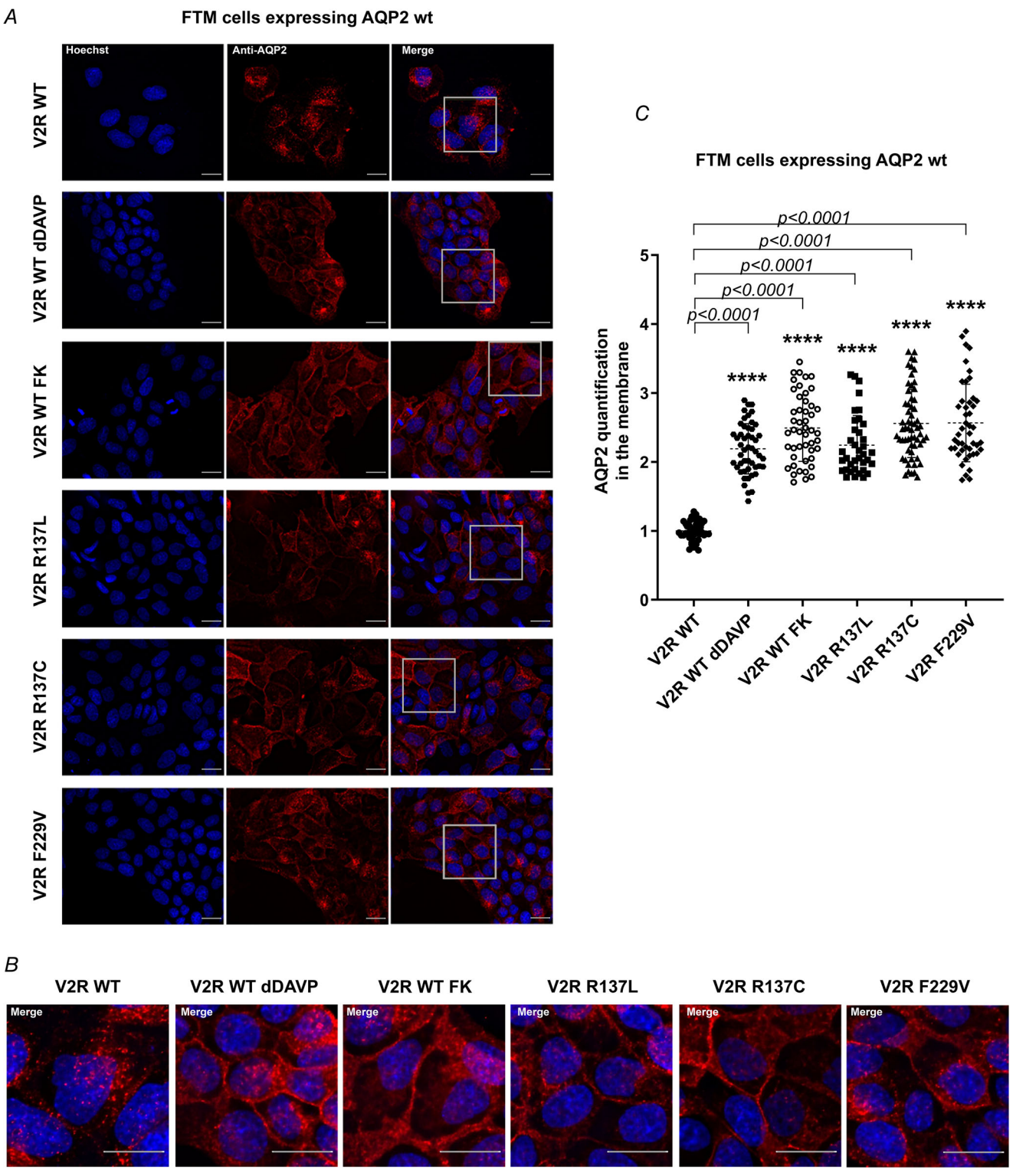

Figure 3. AQP2-wt cell surface localization in FTM cells expressing V2R-WT, V2R-R137L, V2R-R137C and V2R-F229V

A, FTM cells were stained for AQP-wt (red) and nuclei (blue) as indicated. Scale bars: 20 μm. *B*, cells marked by grey squares in *A* were magnified $\times$10 to visualize the subcellular localization of AQP2-wt. Scale bars: 20 μm. *C*, quantification of AQP2-wt protein abundance in the plasma membrane by ImageJ Fiji software. The data are normalized and compared with V2R-WT AQP2-wt abundance and are represented as the means (SD) of five independent experiments. (****$P < 0.0001$ *vs*. V2R-WT).

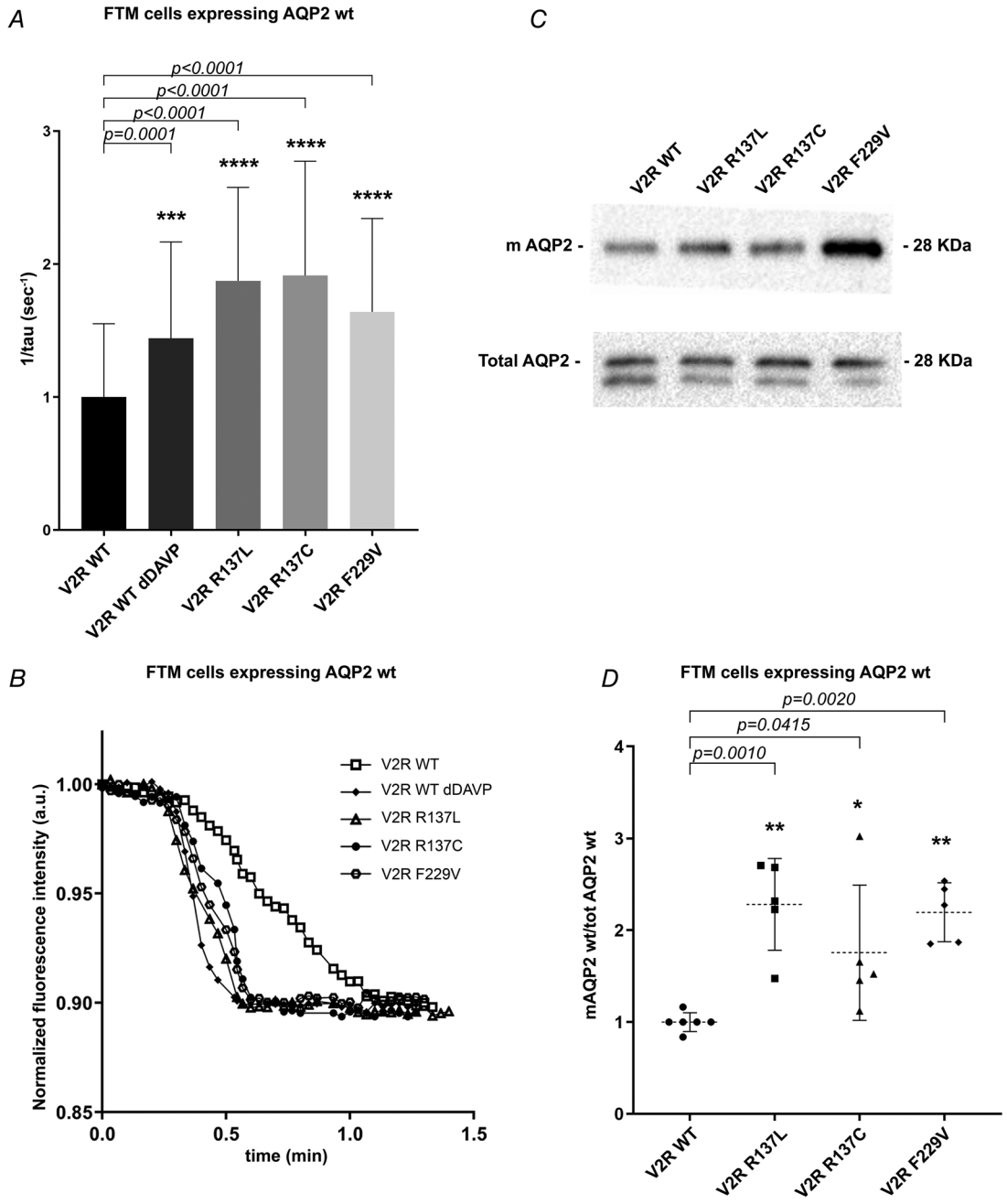

Figure 4. Osmotic water permeability and AQP2-wt membrane abundance in FTM cells expressing V2R-WT, V2R-R137L, V2R-R137C and V2R-F229V

A, the temporal osmotic response is indicated as $1/\tau$. The data are normalized to V2R-WT and are represented as the means (SD) of five independent experiments (***$P < 0.001$, ****$P < 0.0001$ *vs*. V2R-WT). *B*, representative normalized traces of the time course of alteration in the osmotic water permeability in response to exposure to a hyperosmotic solution, followed by modulation of normalized calcein fluorescence intensity. *C*, representative western blots of the FTM plasma membrane-enriched fraction probed with AQP2 antibodies (mAQP2) and compared with total AQP2 (Total AQP2). *D*, densitometric analysis of AQP2 bands. The data are normalized and compared with V2R-WT and are represented as the means (SD) of five independent experiments. (*$P < 0.05$, **$P < 0.01$, *vs*. V2R-WT).

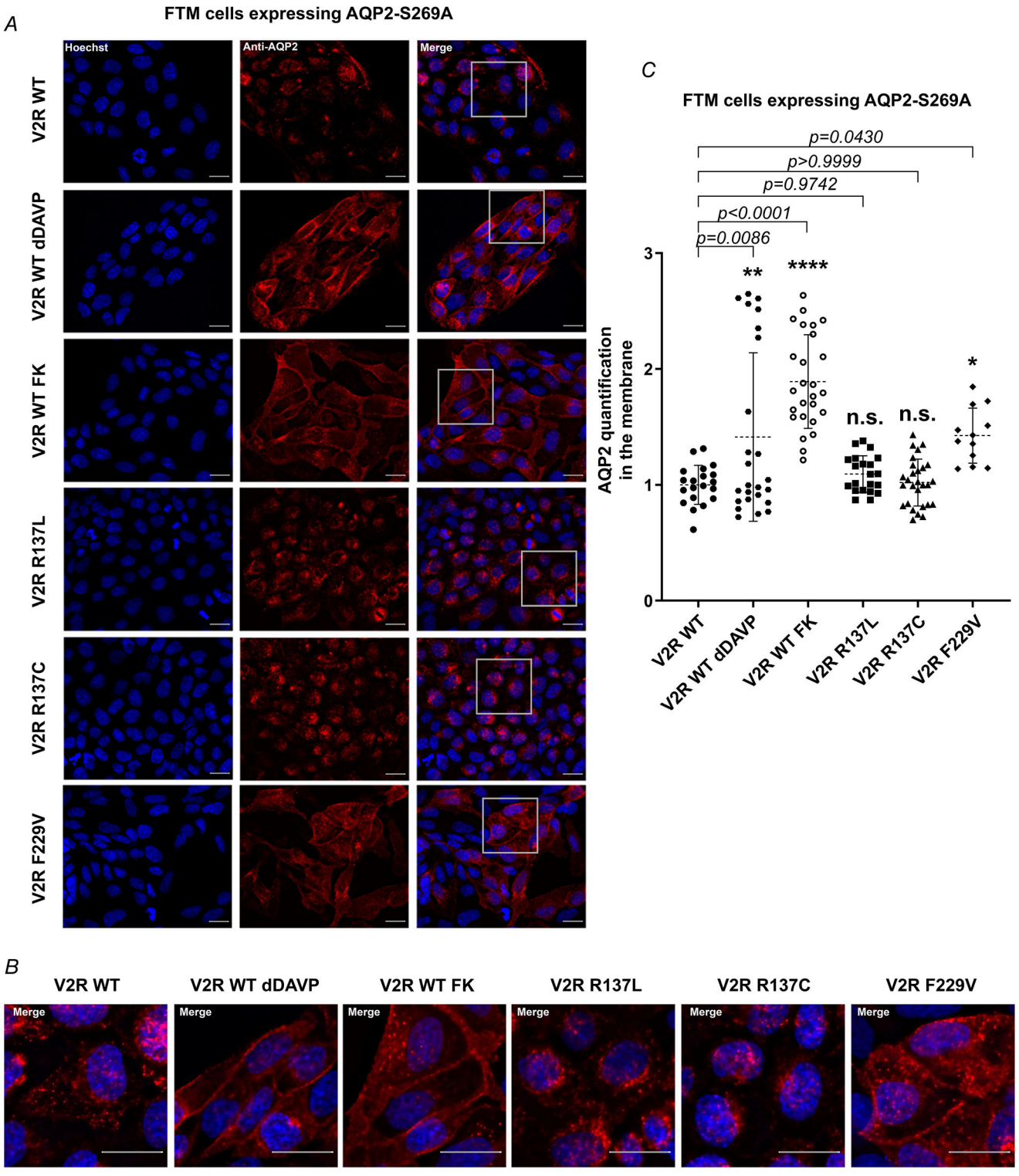

Figure 5. AQP2-S269A cell surface localization in FTM cells expressing V2R-WT, V2R-R137L, V2R-R137C and V2R-F229V

A, FTM cells were stained for AQP-wt (red) and nuclei (blue) as indicated. Scale bars: 20 μm. *B*, cells marked by grey squares in *A* were magnified $\times$10 to visualize the subcellular localization of AQP2-S269A. Scale bars: 20 μm. *C*, quantification of AQP2-S269A protein abundance in the plasma membrane was obtained using the ImageJ Fiji software. The data are normalized to V2R-WT AQP2-S269A abundance and are represented as the means (SD) of three independent experiments (*$P < 0.05$, **$P < 0.01$, ****$P < 0.0001$, n.s. *vs*. V2R-WT).

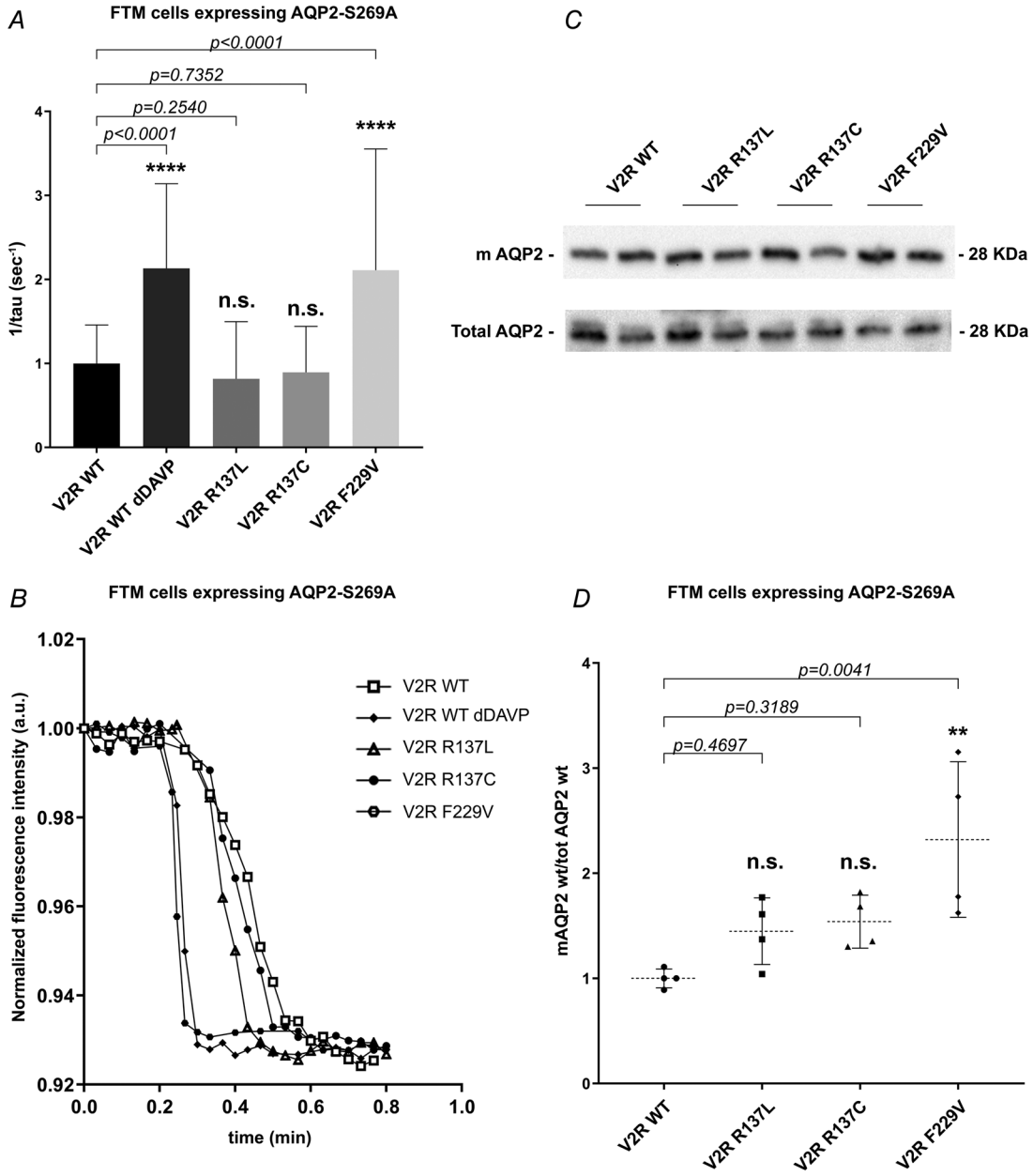

Figure 6. Osmotic water permeability and AQP2-S269A membrane abundance in FTM cells expressing V2R-WT, V2R-R137L, V2R-R137C and V2R-F229V
A, the temporal osmotic response is indicated as $1/\tau$. The data are normalized to V2R-WT and are represented as the means (SD) of three independent experiments (****$P < 0.0001$, n.s. *vs*. V2R-WT). *B*, representative normalized traces of the time course of alteration in the osmotic water permeability in response to exposure to a hyper-osmotic solution, followed by modulation of normalized calcein fluorescence intensity. *C*, representative western blots of FTM cells showing membrane-bound AQP2 (mAQP2) and total AQP2 (Total AQP2) immunoreactivity. *D*, densitometric analysis of AQP2-S269A immunoreactivity of plasma membrane-enriched fractions (mAQP2) normalized to the total AQP2 (totAQP2) in FTM cells expressing the V2R-WT or the constitutively active mutants -R137L, -R137C and -F229V. The data are normalized to V2R-WT and represented as the means (SD) of four independent experiments (**$P < 0.01$, n.s. *vs*. V2R-WT).

AQP2-S269A accumulation to the plasma membrane. As a control, the V2R-WT cell line exposed to dDAVP had a significantly higher temporal osmotic response (reported as $1/\tau$) compared with untreated cells [Fig. 6*A* and *B*; V2R-WT, 1.000 (0.4585), $n = 3$ independent experiments, 137 cells tested; V2R-WT dDAVP, 2.132 (1.008), $n = 3$ independent experiments, 45 cells tested; V2R-R137L, 0.8167 (0.6803), $n = 3$ independent experiments, 164 cells

tested; V2R-R137C, 0.8938 (0.5481), $n = 3$ independent experiments, 201 cells tested; and V2R-F229V, 2.109 (1.444), $n = 3$ independent experiments, 84 cells tested].

Abundance of AQP2-S269A on the plasma membrane was also evaluated by western blotting analysis of plasma membrane-enriched preparations. In comparison to unstimulated V2R-WT-expressing cells, the membrane abundance of AQP2-S269A was not significantly different in cells expressing the V2R-R137L or V2R-R137C mutants, whereas in V2R-F229V-expressing cells, the relative abundance of AQP2-S269A was significantly higher, indicating that in this mutant the receptor was still constitutively active [Fig. 6*C* and *D*; V2R-WT, 1.000 (0.08936); V2R-R137L, 1.448 (0.3166); V2R-R137C, 1.540 (0.2521); and V2R-F229V, 2.321 (0.7402); $n = 4$ independent experiments].

Role of pS256 or pS269 AQP2 phosphorylation site in the cells expressing V2R mutants

The different distributions of AQP2 observed in V2R-F229V- compared with V2R-R137L/C-expressing cells with the AQP2-S269A phospho-mimicking mutant suggests differences in the AQP2 signalling pathway. To investigate the importance of the S256 *versus* S269 sites, FTM cells expressing AQP2-S256A, which cannot be phosphorylated at S256, were stably transfected with the different receptors.

As shown in Fig. 7*A*, the widefield microscopy with deconvolution analysis revealed that in V2R-F229V-expressing cells, AQP2-S256A is predominately located in intracellular compartments, showing a similar subcellular localization to that observed in V2R-WT-expressing cells exposed to dDAVP or FK in V2R-WT, supporting the hypothesis that AQP2 phosphorylation at S256 is necessary for the insertion of AQP2 into the plasma membrane. In contrast, V2R-R137L and V2R-R137C still displayed a marked accumulation of AQP2 into the plasma membrane, indicating that these mutant-expressing cells retain the gain-of-function phenotype even if the S256 cannot be phosphorylated. Representative ×10 magnified images are shown in Fig. 7*B*. The statistical analysis of quantified AQP2-S256A membrane abundance in each of the cell lines is shown in Fig. 7*C* [V2R-WT, 1.000 (0.1299), $n = 3$ independent experiments, 25 cells tested; V2R-WT dDAVP, 0.9521 (0.1408), $n = 3$ independent experiments, 30 cells tested; V2R-WT FK, 0.9905 (0.1256), $n = 3$ independent experiments, 23 cells tested; V2R-R137L, 2.047 (0.4815), $n = 3$ independent experiments, 20 cells tested; V2R-R137C, 1.777 (0.3537), $n = 3$ independent experiments, 34 cells tested; and V2R-F229V, 0.918 (0.1710), $n = 3$ independent experiments, 30 cells tested].

Next, we performed video imaging experiments in FTM cells expressing AQP2-S256A to test the effect of AQP2-S256A on the time course of the osmotic water permeability.

Cells expressing the active V2R-F229V had a similar temporal osmotic response (reported as $1/\tau$) to the V2R-WT cells. In V2R-WT-expressing cells co-expressed with AQP2-S256A, no increase in osmotic water permeability in response to dDAVP was observed, indicating that the S256-AQP2 phosphorylation site is essential in AQP2 translocation and insertion into the plasma membrane in these cells. Conversely, as expected for V2R-R137L- and V2R-R137C-expressing cells, the basal value of the temporal osmotic response was significantly higher with respect to cells expressing V2R-WT, indicating that V2R-R137L and V2R-R137C signal through an alternative PKA-independent pathway, not requiring an intact S256 in the AQP2 water channel [Fig. 8*A* and *B*; V2R-WT, 1.000 (0.5024), $n = 5$ independent experiments, 280 cells tested; V2R-WT dDAVP, 1.024 (0.5686), $n = 5$ independent experiments, 242 cells tested; V2R-R137L, 2.34 (1.593), $n = 5$ independent experiments, 71 cells tested; V2R-R137C, 2.124 (1.537), $n = 5$ independent experiments, 217 cells tested; and V2R-F229V, 1.041 (0.5879), $n = 5$ independent experiments, 163 cells tested].

Role of Rho-associated kinase (ROCK) in V2R-R137L and R137C signalling

We recently demonstrated (Ranieri et al., 2020) that Rho-associated kinase (ROCK) phosphorylates S/T269-AQP2 *in vitro* and that this phosphorylation was almost completely prevented in the presence of the ROCK inhibitor Y27632. Moreover, we provided evidence that ROCK is responsible for the high pS/T269-AQP2 levels in cells expressing V2R-R137L and V2R-R137C. To confirm these observations, we performed osmotic water permeability measurements in FTM cells expressing V2R-WT and the constitutively active V2R-R137L, V2R-R137C and V2R-F229V mutants in the presence of the ROCK inhibitor Y27632.

As shown in Fig. 9*A* and *B*, in cells expressing all the constitutively active mutants, the temporal osmotic response was significantly higher compared with cells expressing the V2R-WT [V2R-R137L, 1.877 (0.9498), $n = 6$ independent experiments, 165 cells tested; V2R-R137C, 1.920 (0.9684), $n = 6$ independent experiments, 136 cells tested; V2R-F229V, 1.885 (0.8893), $n = 6$ independent experiments, 133 cells tested; and V2R-WT, 1.000 (0.5321), $n = 6$ independent experiments, 148 cells tested].

Interestingly, pretreatment with the ROCK inhibitor Y27632 significantly reduced the higher osmotic response

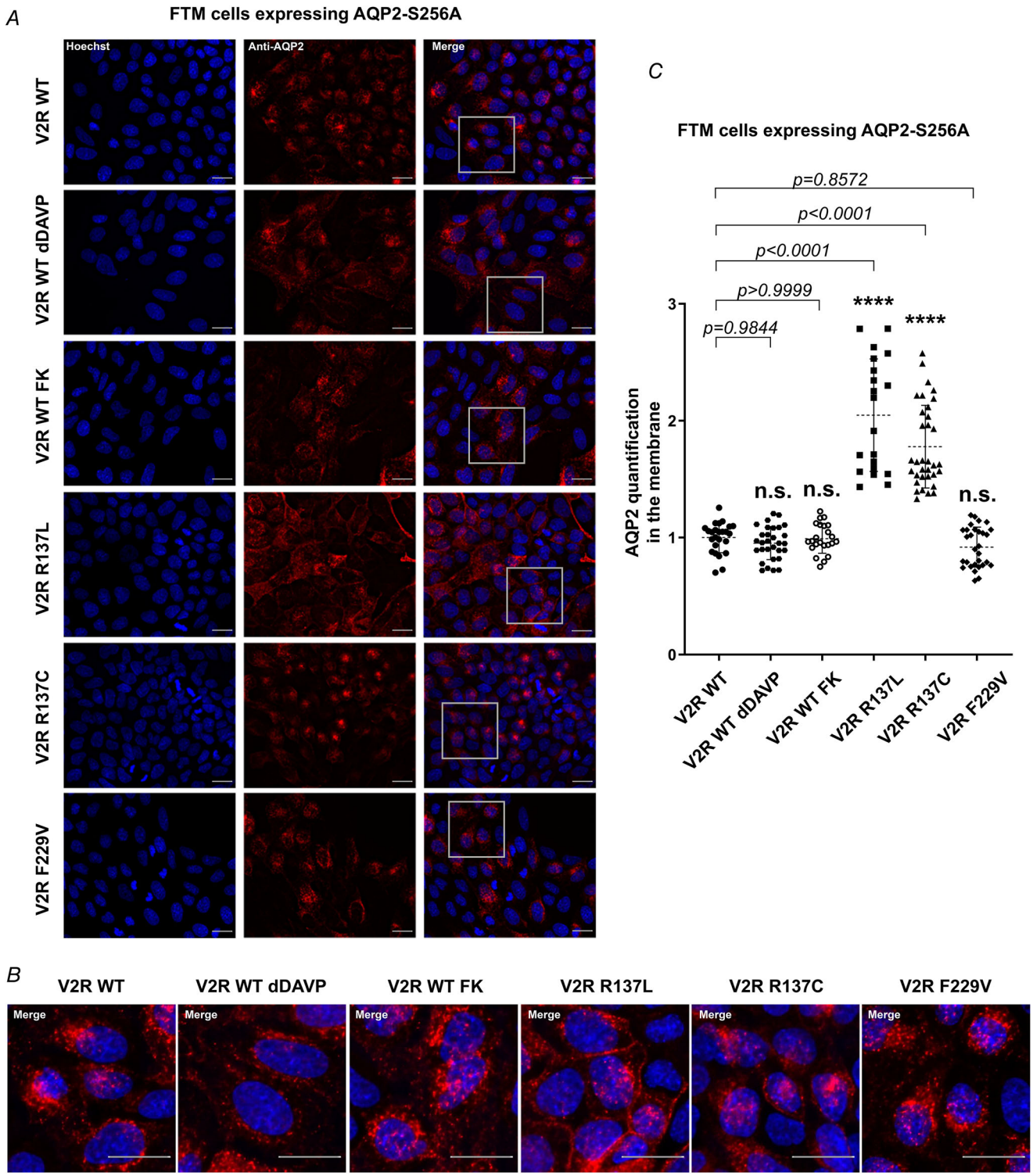

Figure 7. AQP2-S256A localization in FTM cells expressing V2R-WT, V2R-R137L, V2R-R137C and V2R-F229V

A, FTM cells were stained for AQP-S256A (red) and nuclei (blue) as indicated. Scale bars: 20 μm. *B*, cells marked by grey squares in *A* were magnified $\times$10 to visualize the subcellular localization of AQP2-S256A. Scale bars: 20 μm. *C*, quantification of AQP2-S256A protein abundance in the plasma membrane was performed using ImageJ Fiji software. The data are normalized and compared with V2R-WT AQP2-S256A abundance and are represented as the means (SD) of three independent experiments (****$P < 0.0001$, n.s. *vs*. V2R-WT).

only in V2R-R137L and V2R-R137C mutants, indicating that these two mutant receptors were sensitive to the ROCK inhibitor Y27632 [V2R-R137L + Y27632, 1.246 (0.5830), $n = 6$ independent experiments, 92 cells tested *vs*. V2R-R137L, 1.877 (0.9498), $n = 6$ independent experiments, 165 cells tested; V2R-R137C + Y27632, 1.221 (0.5772), $n = 6$ independent experiments, 153 cells tested *vs*. V2R-R137C, 1.920 (0.9684), $n = 6$ independent experiments, 136 cells tested]. Y27632 had no effect in cells expressing the V2R-F229V mutant [V2R-F229V + Y27632, 1.771 (0.7340), $n = 6$ independent experiments, 94 cells tested *vs*. V2R-F229V, 1.885 (0.8893), $n = 6$ independent experiments, 133 cells tested]. The sole exposure of V2R-WT cells to Y27632 increased the osmotic water permeability in the absence of hormonal stimulation, in agreement with previous findings [Tamma et al., 2001; Fig. 9*A* and *B*; V2R-WT + Y27632, 1.571 (0.8876), $n = 6$ independent experiments, 166 cells tested *vs*. V2R-WT, 1.000 (0.5321), $n = 6$ independent experiments, 148 cells tested].

We next evaluated the basal activity of the enzyme ROCK by monitoring the phosphorylation of the downstream protein substrate myosin phosphatase target 1 (MYPT1) at Thr696. Western blotting analysis revealed that, compared with V2R-WT, V2R-R137L- and V2R-R137C-expressing cells presented a significant increase in pT696-MYPT1 levels. In contrast, no difference was observed in the V2R-F229V mutant with respect to V2R-WT [Fig. 10*A* and *B*; V2R-WT, 1.000 (0.253); V2R-R137L, 2.022 (0.6288); V2R-R137C, 2.290 (0.5198); and V2R-F229V, 1.281 (0.4348); $n = 5$ independent experiments].

Of note, this significantly higher ROCK activity was abolished in V2R-R137L and V2R-R137C cells expressing the AQP2-S269A mutant, showing no difference in ROCK activity with respect to V2R-WT [V2R-WT, 1.000 (0.2481); V2R-R137L, 0.8865 (0.2776); V2R-R137C, 0.9348 (0.4136); V2R-F229V, 0.7574 (0.2326); $n = 5$ independent experiments]. These data confirm the involvement of ROCK as a kinase responsible for pS/T269-AQP2 phosphorylation (Fig. 10*C* and *D*].

Discussion

Nephrogenic syndrome of inappropriate antidiuresis is associated with gain-of-function mutations of the V2R, characterized by the inability to excrete a free water load, hyponatraemia and undetectable circulating levels of vasopressin. Since its discovery (Feldman et al., 2005), only a few cases have been described (Decaux et al., 2007; Miyado et al., 2019; Ranieri et al., 2019; Tiulpakov et al., 2016) and among them, V2R-R137C was found to be the most frequent mutation (Carpentier et al., 2012; Erdélyi et al., 2015).

The optimal therapy for NSIAD patients would be the use of vaptans; however, although tolvaptan was effective in silencing the constitutive signalling activity of the V2R-F229V mutant receptor *in vitro*, *in vivo* data

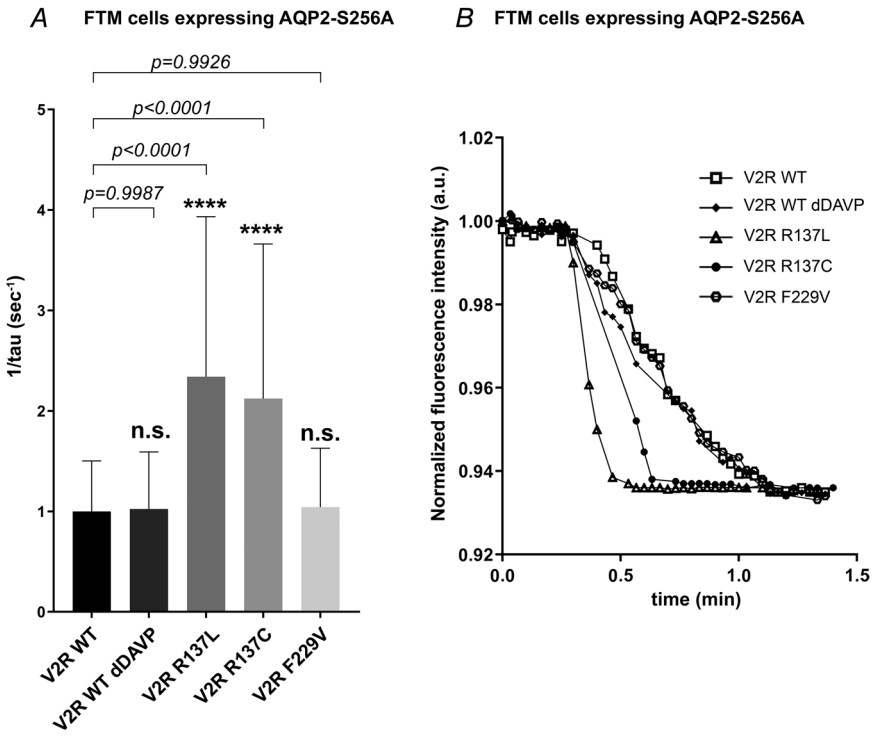

Figure 8. Osmotic water permeability in FTM cells expressing AQP2-S256A and V2R-WT, V2R-R137L, V2R-R137C and V2R-F229V
A, the temporal osmotic response is indicated as $1/\tau$. The data are normalized to V2R-WT and are represented as the means (SD) of five independent experiments (****$P < 0.0001$, n.s. *vs*. V2R-WT). *B*, representative normalized traces of the time course of alteration in the osmotic water permeability in response to exposure to a hyperosmotic solution, followed by modulation of normalized calcein fluorescence intensity.

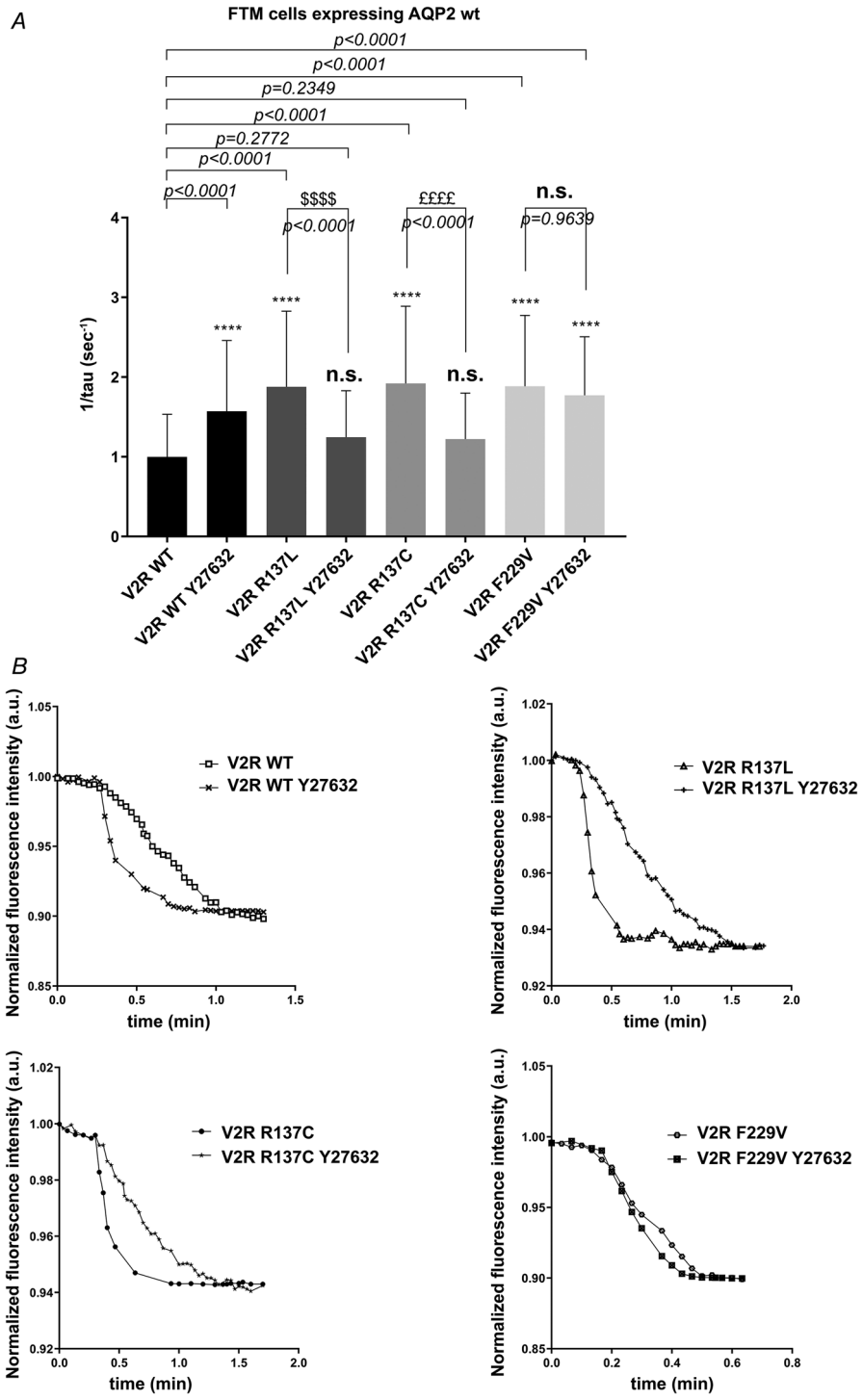

Figure 9. Osmotic water permeability in FTM cells expressing AQP2-WT and V2R-WT or constitutively active mutants V2R-R137L, V2R-R137C and V2R-F229V

A, the temporal osmotic response is indicated as $1/\tau$. The data are normalized to V2R-WT and are represented as the means (SD) of six independent experiments ($^{****}P < 0.0001$ *vs*. V2R-WT; $^{\$\$\$\$}P < 0.0001$ *vs*. V2R-RL; $^{££££}P < 0.0001$, n.s. *vs*. V2R-WT or V2R-FV). *B*, representative normalized traces of the time course of alteration in the osmotic water permeability in response to exposure to a hyperosmotic solution, followed by modulation of normalized calcein fluorescence intensity.

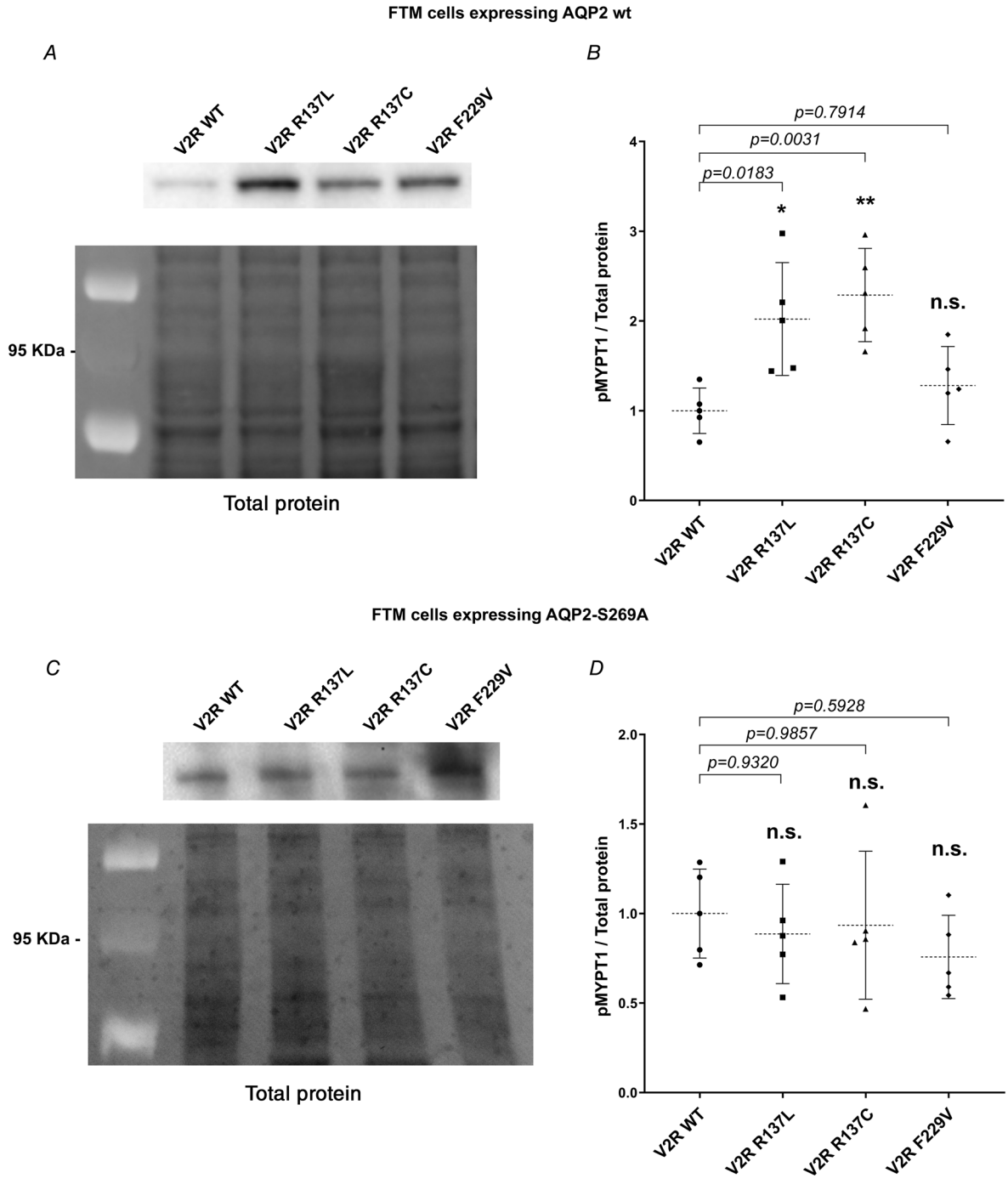

Figure 10. Densitometric analysis of pT696-MYPT1 immunoreactive bands normalized to total protein in FTM cells expressing AQP2-wt or AQP2-S269A and wild-type or constitutive V2R
A, representative western blots of FTM cells expressing AQP2-wt, showing pT696-MYPT1 immunoreactivity. *B*, densitometric analysis of pT696-MYPT1 immunoreactivity normalized to total protein in FTM cells expressing AQP2-wt and V2R-WT or constitutively active mutants -R137L, -R137C and -F229V. The data, normalized to V2R-WT, are expressed as means (SD) of five experiments (*$P < 0.05$, **$P < 0.001$, n.s. *vs*. V2R-WT). *C*, representative western blots of FTM cells expressing AQP2-S269A, showing pT696-MYPT1 immunoreactivity. *D*, densitometric analysis of pT696-MYPT1 bands normalized to total protein in FTM cells expressing AQP2-S269A and V2R-WT or constitutively active mutants -R137L, -R137C and -F229V. The data, normalized to V2R-WT, are expressed as means (SD) of five experiments (n.s. *vs*. V2R-WT).

have shown that V2R-R137L/C did not respond to the administration of V2R antagonists (Carpentier et al., 2012; Erdélyi et al., 2015; Ranieri et al., 2019; Tiulpakov et al., 2016).

The present study was undertaken to dissect the signalling associated with V2R-R137L/C mutants compared with V2R-F229V. We have recently demonstrated that in renal cells expressing three distinct gain-of-function V2R mutations (V2R-R137L, V2R-R137C and V2R-F229V), AQP2 displayed constitutive trafficking to the plasma membrane in the absence of vasopressin stimulation that was independent of the cAMP/PKA signalling pathway in V2R-R137L/C mutants (Ranieri et al., 2019, 2020). Moreover, V2R-R137L and V2R-R137C mutants had significantly higher basal pT269-AQP2 levels that were reduced by treatment with ROCK inhibitor, which also reduced the elevated basal osmotic water permeability.

In the present study, we advanced the investigation of this alternative PKA-independent pathway observed in V2R-R137L- and V2R-R137C-expressing cells. To this end, we took advantage of the use of renal cell culture models, FTM cells, stably transfected with V2R mutants (V2R-R137L, V2R-R137C and V2R-F229V) and AQP2-wt or non-phosphorylatable AQP2-S269A/AQP2-S256A.

The obtained results can be summarized as follows: (i) disruption of the S269 phosphorylation site prevented the constitutive trafficking of AQP2 to the plasma membrane and reduced the osmotic water permeability in cells expressing V2R-R137L/C mutants; (ii) in these cells, a significant reduction in ROCK activity was observed, indicating that the gain-of-function phenotype depends on AQP2 phosphorylation at S269; (iii) V2R-R137L/C mutants retained the gain-of-function phenotype when AQP2-S256A was co-expressed, indicating that the phosphorylation at S256 had no influence on AQP2 translocation, consistent with a cAMP/PKA-independent pathway; and (iv) cells expressing V2R-F229V mutant and the non-phosphorylatable AQP2-S256A lost their gain-of-function phenotype, indicating that, instead, this mutant requires an intact S256 phosphorylation site for translocation.

The different behaviours of the V2R variants might be attributable to the distinct sites of the mutations, given that V2R-R137L/C affects the conserved DRY/H motif in the second intracellular loop on the vasopressin receptor (Carpentier et al., 2012; Feldman et al., 2005), whereas the mutation V2R-F229V is located in the third intracellular loop of V2R (Carpentier et al., 2012). The DRY/H motif plays a crucial role in the stabilization of the receptor in its constitutive active or inactive form (Audet & Bouvier, 2012). Substitution of the arginine for histidine (V2R-R137H) causes a loss of function of the V2R, resulting in an opposite disease, the Nephrogenic Diabetes Insipidus (NDI). By structural modelling, it has been reported that V2R-R137L mutation switches the receptor into an activated form independent of vasopressin binding (Powlson et al., 2016).

These different mutations are associated with different signalling pathways activated by these receptors, but leading to constitutive AQP2 relocation to the plasma membrane. Nevertheless, although all three mutations tested (V2R-R137L, V2R-R137C and V2R-F229V) have constitutively elevated osmotic water permeability, specific inhibition of PKA does not affect the basal osmotic water permeability in V2R-R137L and V2R-R137C mutants, whereas it does in V2R-F229V mutant-expressing cells (Ranieri et al., 2020). Regarding the importance of AQP2 phosphorylation in this context, previous reports showed that phosphorylation at S256 precedes phosphorylation of other serine residues within the AQP2 C-terminus (Hoffert et al., 2006; Moeller et al., 2010). Among these serines, S269 phosphorylation is thought to be crucial for membrane retention of AQP2 (Hoffert et al., 2008; Moeller et al., 2009), and recent studies highlight the importance of S269 phosphorylation in AQP2 tracking independently of S256 phosphorylation (Ando et al., 2016; Cheung et al., 2019).

The kinase committed to phosphorylate the S/T269 is not known; however, PKA does not phosphorylate this site *in vitro* (Hoffert et al., 2008). Based on the observation that S/T269 in AQP2 lies within a ROCK phosphorylation motif, RXS/T (Ando et al., 2016), we previously demonstrated that G12/13–Rho–ROCK signalling is activated in V2R-R137L, and this pathway is responsible for the constitutively higher AQP2 cell surface abundance and osmotic water permeability (Ranieri et al., 2020).

In a different renal cell culture model, in the present work, we provide direct evidence that disruption of the S269 phosphorylation site prevents the constitutive trafficking of AQP2 to the plasma membrane and reduces the osmotic water permeability in cells expressing V2R-R137L/C mutants. Interestingly, the V2R-R137L/C mutants cells display significantly higher ROCK activity (compared with V2R-WT-expressing cells), whereas in V2R-R137L/C mutants transfected with the non-phosphorylatable S269A, a significant reduction in ROCK activity was observed, indicating that the gain-of-function phenotype depends on AQP2-S269 phosphorylation, probably owing to ROCK activity. Confirmation of the independence of this pathway from the S256 phosphorylation site comes from the observation that V2R-R137L/C mutants retained the gain-of-function phenotype when AQP2-S256A was co-expressed, indicating that the phosphorylation at S256 had no influence on AQP2 translocation, consistent with a cAMP/PKA-independent pathway. Conversely, in cells expressing the V2R-F229V mutant and the non-phosphorylatable AQP2-S256A, the

gain-of-function phenotype disappears, indicating that, instead, this mutant requires an intact S256 phosphorylation site.

Moreover, the observation that ROCK inhibition did not affect the gain-of-function phenotype in V2R-F229V-expressing cells further confirms that V2R-R137L/C and V2R-F229V activate distinct intracellular pathways to promote AQP2 relocation to the plasma membrane. In this study, we were not able to identify the ROCK isoform (ROCK1 or ROCK2) involved. However, it is known that ROCK1 and ROCK2 isoforms display 92% homology at the kinase domain. The identification of the ROCK isoform involved or whether other kinases might be implicated in AQP2-S269 phosphorylation needs further investigation.

Our findings imply that the V2R-R137L/C variant of the V2R activates a hitherto-unrecognized, compartmentalized signalling pathway acting downstream to G-protein-coupled receptors, intersecting the system controlling AQP2 trafficking.

Members of the vasopressin receptor family couple to different subsets of G-proteins (Liu & Wess, 1996), and we have shown a functional interaction of V2R with G12/13, demonstrating that the gain-of-function variant V2R-R137L directly or indirectly activates the G12/13–Rho–ROCK signalling pathway (Ranieri et al., 2020). The importance of ROCK in V2R-R137L/C signalling is confirmed by the present data showing that treatment with ROCK inhibitor reduces the constitutively high osmotic water permeability to the level of V2R-WT-expressing cells.

The physiological agonist of V2R is vasopressin, a peptide very similar to oxytocin, and the two G-protein-coupled receptors display a high degree of homology and can form heterodimers (Devost & Zingg, 2004; Muratspahić et al., 2020). Interestingly, it has been shown that oxytocin activates the Rho–ROCK pathway to phosphorylate the regulatory subunit of myosin light chain (MLC), leading to contractions (Moore et al., 2000; Shmygol et al., 2006), and vasopressin can also induce uterine contractions (Maggi et al., 1990).

Therefore, it can be speculated that the gain-of-function variant V2R-R137L locks the receptor in a configuration able to activate, either directly or indirectly, a 'non-canonical' G12/13–Rho–ROCK signalling pathway that leads to AQP2 phosphorylation at S/T269 and a constitutive increase in the osmotic water permeability, which translates into the pathological outcome of NSIAD. Whether the activation of this pathway might explain other, much more frequent conditions characterized by water retention associated with elevated pS/T269-AQP2 levels independently from activation of the classical PKA-dependent phosphorylation of AQP2 at S256 remains to be determined.

As a general consideration, the physiological relevance of such versatility in signalling associated with V2R variants causing NSIAD has potential importance for efficient targeting of the V2R/AQP2 pathway for a therapeutic intervention in this rare genetic kidney disease.

References

Ando, F., Sohara, E., Morimoto, T., Yui, N., Nomura, N., Kikuchi, E., Takahashi, D., Mori, T., Vandewalle, A., Rai, T., Sasaki, S., Kondo, Y., & Uchida, S. (2016). Wnt5a induces renal AQP2 expression by activating calcineurin signalling pathway. *Nature Communications*, **7**(1), 13636.

Audet, M., & Bouvier, M. (2012). Restructuring G-protein-coupled receptor activation. *Cell*, **151**(1), 14–23.

Carpentier, E., Greenbaum, L. A., Rochdi, D., Abrol, R., Goddard, W. A., Bichet, D. G., & Bouvier, M. (2012). Identification and characterization of an activating F229V substitution in the V2 vasopressin receptor in an infant with NSIAD. *Journal of the American Society of Nephrology*, **23**(10), 1635–1640.

Cheung, P. W., Terlouw, A., Janssen, S. A., Brown, D., & Bouley, R. (2019). Inhibition of non-receptor tyrosine kinase Src induces phosphoserine 256-independent aquaporin-2 membrane accumulation. *The Journal of Physiology*, **597**(6), 1627–1642.

Decaux, G., Vandergheynst, F., Bouko, Y., Parma, J., Vassart, G., & Vilain, C. (2007). Nephrogenic syndrome of inappropriate antidiuresis in adults: High phenotypic variability in men and women from a large pedigree. *Journal of the American Society of Nephrology*, **18**(2), 606–612.

Devost, D., & Zingg, H. H. (2004). Homo- and hetero-dimeric complex formations of the human oxytocin receptor. *Journal of Neuroendocrinology*, **16**(4), 372–377.

Erdélyi, L. S., Mann, W. A., Morris-Rosendahl, D. J., Groß, U., Nagel, M., Várnai, P., Balla, A., & Hunyady, L. (2015). Mutation in the V2 vasopressin receptor gene, AVPR2, causes nephrogenic syndrome of inappropriate diuresis. *Kidney International*, **88**(5), 1070–1078.

Ernstsen, C. V., Login, F. H., Schelde, A. S. B., Therkildsen, J. R., Møller-Jensen, J., Nørregaard, R., Prætorius, H., & Nejsum, L. N. (2022). Acute pyelonephritis: Increased plasma membrane targeting of renal aquaporin-2. *Acta Physiologica (Oxf)*, **234**(2), e13760.

Feldman, B. J., Rosenthal, S. M., Vargas, G. A., Fenwick, R. G., Huang, E. A., Matsuda-Abedini, M., Lustig, R. H., Mathias, R. S., Portale, A. A., Miller, W. L., & Gitelman, S. E. (2005). Nephrogenic syndrome of inappropriate antidiuresis. *New England Journal of Medicine*, **352**(18), 1884–1890.

Fenton, R. A., Pedersen, C. N., & Moeller, H. B. (2013). New insights into regulated aquaporin-2 function. *Current Opinion in Nephrology and Hypertension*, **22**(5), 551–558.

Fushimi, K., Sasaki, S., & Marumo, F. (1997). Phosphorylation of serine 256 is required for cAMP-dependent regulatory exocytosis of the aquaporin-2 water channel. *Journal of Biological Chemistry*, **272**(23), 14800–14804.

Hoffert, J. D., Fenton, R. A., Moeller, H. B., Simons, B., Tchapyjnikov, D., McDill, B. W., Yu, M. J., Pisitkun, T., Chen, F., & Knepper, M. A. (2008). Vasopressin-stimulated increase in phosphorylation at Ser269 potentiates plasma membrane retention of aquaporin-2. *Journal of Biological Chemistry*, **283**(36), 24617–24627.

Hoffert, J. D., Pisitkun, T., Wang, G., Shen, R. F., & Knepper, M. A. (2006). Quantitative phosphoproteomics of vasopressin-sensitive renal cells: Regulation of aquaporin-2 phosphorylation at two sites. *PNAS*, **103**(18), 7159–7164.

Holst, M. R., & Nejsum, L. N. (2019). A versatile aquaporin-2 cell system for quantitative temporal expression and live cell imaging. *American Journal of Physiology Renal Physiology*, **317**(1), F124–F132.

Katsura, T., Gustafson, C. E., Ausiello, D. A., & Brown, D. (1997). Protein kinase A phosphorylation is involved in regulated exocytosis of aquaporin-2 in transfected LLC-PK1 cells. *American Journal of Physiology*, **272**(6), F816-F822.

Liu, J., & Wess, J. (1996). Different single receptor domains determine the distinct G protein coupling profiles of members of the vasopressin receptor family. *Journal of Biological Chemistry*, **271**(15), 8772–8778.

Login, F. H., Jensen, H. H., Pedersen, G. A., Koffman, J. S., Kwon, T. H., Parsons, M., & Nejsum, L. N. (2019). Aquaporins differentially regulate cell-cell adhesion in MDCK cells. *Faseb Journal*, **33**(6), 6980–6994.

Login, F. H., Palmfeldt, J., Cheah, J. S., Yamada, S., & Nejsum, L. N. (2021). Aquaporin-5 regulation of cell-cell adhesion proteins: an elusive "tail" story. *American Journal of Physiology Cell Physiology*, **320**(3), C282–C292.

Maggi, M., delCarlo, P., Fantoni, G., Giannini, S., Torrisi, C., Casparis, D., Massi, G., & Serio, M. (1990). Human myometrium during pregnancy contains and responds to V1 vasopressin receptors as well as oxytocin receptors. *Journal of Clinical Endocrinology and Metabolism*, **70**(4), 1142–1154.

Miyado, M., Fukami, M., Takada, S., Terao, M., Nakabayashi, K., Hata, K., Matsubara, Y., Tanaka, Y., Sasaki, G., Nagasaki, K., Shiina, M., Ogata, K., Masunaga, Y., Saitsu, H., & Ogata, T. (2019). Germline-derived gain-of-function variants of GSA-coding GNAS gene identified in nephrogenic syndrome of inappropriate antidiuresis. *Journal of the American Society of Nephrology*, **30**(5), 877–889.

Moeller, H. B., Knepper, M. A., & Fenton, R. A. (2009). Serine 269 phosphorylated aquaporin-2 is targeted to the apical membrane of collecting duct principal cells. *Kidney International*, **75**(3), 295–303.

Moeller, H. B., Praetorius, J., Rützler, M. R., & Fenton, R. A. (2010). Phosphorylation of aquaporin-2 regulates its endocytosis and protein-protein interactions. *PNAS*, **107**(1), 424–429.

Moore, F., da Silva, C., Wilde, J. I., Smarason, A., Watson, S. P., & López Bernal, A. (2000). Up-regulation of p21- and RhoA-activated protein kinases in human pregnant myometrium. *Biochemical and Biophysical Research Communications*, **269**(2), 322–326.

Muratspahić, E., Monjon, E., Duerrauer, L., Rogers, S. M., Cullen, D. A., vanden Broeck, J., & Gruber, C. W. (2020). Oxytocin/vasopressin-like neuropeptide signaling in insects. *Vitamins and Hormones*, **113**, 29–53.

Nejsum, L. N., Christensen, T. M., Robben, J. H., Milligan, G., Deen, P. M. T., Bichet, D. G., & Levin, K. (2011). Novel mutation in the AVPR2 gene in a Danish male with nephrogenic diabetes insipidus caused by ER retention and subsequent lysosomal degradation of the mutant receptor. *NDT Plus*, **4**(3), 158–163.

Nielsen, S., Smith, B. L., Christensen, E. I., Knepper, M. A., & Agre, P. (1993). CHIP28 water channels are localized in constitutively water-permeable segments of the nephron. *Journal of Cell Biology*, **120**(2), 371–383.

Powlson, A. S., Challis, B. G., Halsall, D. J., Schoenmakers, E., & Gurnell, M. (2016). Nephrogenic syndrome of inappropriate antidiuresis secondary to an activating mutation in the arginine vasopressin receptor AVPR2. *Clinical Endocrinology*, **85**(2), 306–312.

Ranieri, M., di Mise, A., Tamma, G., & Valenti, G. (2019). Vasopressin–aquaporin-2 pathway: Recent advances in understanding water balance disorders, version1, F1000Res. https://doi.org/10.12688/f1000research.16654.1

Ranieri, M., Venneri, M., Pellegrino, T., Centrone, M., di Mise, A., Cotecchia, S., Tamma, G., & Valenti, G. (2020). The vasopressin receptor 2 mutant R137L linked to the nephrogenic syndrome of inappropriate antidiuresis (NSIAD) signals through an alternative pathway that increases AQP2 membrane targeting independently of S256 phosphorylation. *Cells*, **9**(6), 1354.

Rochdi, M. D., Vargas, G. A., Carpentier, E., Oligny-Longpré, G., Chen, S., Kovoor, A., Gitelman, S. E., Rosenthal, S. M., von Zastrow, M., & Bouvier, M. (2010). Functional characterization of vasopressin type 2 receptor substitutions (R137H/C/L) leading to nephrogenic diabetes insipidus and nephrogenic syndrome of inappropriate antidiuresis: implications for treatments. *Molecular Pharmacology*, **77**(5), 836–845.

Schindelin, J., Arganda-Carreras, I., Frise, E., Kaynig, V., Longair, M., Pietzsch, T., Preibisch, S., Rueden, C., Saalfeld, S., Schmid, B., Tinevez, J. Y., White, D. J., Hartenstein, V., Eliceiri, K., Tomancak, P., & Cardona, A. (2012). Fiji: An open-source platform for biological-image analysis. *Nature Methods*, **9**(7), 676–682.

Shmygol, A., Gullam, J., Blanks, A., & Thornton, S. (2006). Multiple mechanisms involved in oxytocin-induced modulation of myometrial contractility. *Acta Pharmacologica Sinica*, **27**(7), 827–832.

Tamma, G., Klussmann, E., Maric, K., Aktories, K., Svelto, M., Rosenthal, W., & Valenti, G. (2001). Rho inhibits cAMP-induced translocation of aquaporin-2 into the apical membrane of renal cells. *American Journal of Physiology Renal Physiology*, **281**(6), F1092–F1101.

Tiulpakov, A., White, C. W., Abhayawardana, R. S., See, H. B., Chan, A. S., Seeber, R. M., Heng, J. I., Dedov, I., Pavlos, N. J., & Pfleger, K. D. G. (2016). Mutations of vasopressin receptor 2 including novel L312S have differential effects on trafficking. *Molecular Endocrinology*, **30**(8), 889–904.

van Balkom, B. W. M., Savelkoul, P. J. M., Markovich, D., Hofman, E., Nielsen, S., van der Sluijs, P., & Deen, P. M. T. (2002). The role of putative phosphorylation sites in the targeting and shuttling of the aquaporin-2 water channel. *Journal of Biological Chemistry*, **277**(44), 41473–41479.

Additional information

Data availability statement

All data supporting the results are in the paper itself. The statistical summary document contains data that support the findings of this study.

Competing interests

None.

Author contributions

The experiments were performed in the following laboratories: Laboratory of Cell Physiology, Department of Biosciences, Biotechnologies and Environment, University of Bari, Bari, Italy; Laboratory of Molecular Pharmacology, National Centre for Drug Research and Evaluation, Istituto Superiore di Sanità, Rome, Italy; and Laboratory of Clinical Cell Biology, Department of Clinical Medicine, Aarhus University, Aarhus, Denmark. M.V., V.V., A.D.M., M.R., M.C., G.T., L.N.N. and G.V. designed and performed the experiments and analysed the data; M.V., L.N.N. and G.V. interpretated the data, wrote the manuscript and read the manuscript critically. All authors have approved the final version of the manuscript and agree to be accountable for all aspects of the work in ensuring that questions related to the accuracy or integrity of any part of the work are appropriately investigated and resolved. All persons designated as authors qualify for authorship, and all those who qualify for authorship are listed.

Funding

This research was funded by Regional project POR Puglia Innonetwork (grant number H6GG787 to G.V.). Marianna Ranieri is supported financially by 'Intervento cofinanziato dal Fondo di Sviluppo e Coesione 2007-2013-APQ Ricerca Regione Puglia, Programma Regionale a Sostegno della Specializzazione Intelligente e della Sostenibilità Sociale ed Ambientale–FutureInResearch' (code CHVNKZ4). Annarita Di Mise is supported by 'Attrazione e Mobilità dei Ricercatori, PON "R&I" 2014—2020, Azione I.2' (code AIM1893457-3, linea 1).

Acknowledgements

The authors would like to thank Thomas Breithebach, Aarhus University, Denmark, for expert technical assistance with deconvolution.

Open Access Funding provided by Universita degli Studi di Bari Aldo Moro within the CRUI-CARE Agreement.

Keywords

AQP2, aquaporin, arginine vasopressin receptor 2, kidney, nephrogenic syndrome of inappropriate antidiuresis, Rho-associated kinase, vasopressin

Supporting information

Additional supporting information can be found online in the Supporting Information section at the end of the HTML view of the article. Supporting information files available:

Statistical Summary Document
Peer Review History